International Journal of
Advanced Thermofluid Research

ISSN 2455-1368
www.ijatr.org

Magnetohydrodynamic Jeffrey Fluid Over a Porous Unsteady Shrinking Sheet with Suction Parameter: Numerical Approach

M. K. Murthy [1], C. S. K. Raju [2], Mohammad Mainul Hoque [3]* and N. N Anika [4]

[1]Department of Mathematics, S.V. University, Tirupati-517502, A.P., India.
[2]Department of Mathematics, VIT University, Vellore-63014, Tamilnadu, India.
[3]Disipline of Chemical Engineering, University of Newcastle, Callaghan-2308, Australia.
[4]Disipline of Mechanical Engineering, University of Newcastle, Callaghan-2308, Australia.

Keywords
MHD •
Jeffrey Parameter •
Unsteady Shrinking Sheet.

Received
March 29, 2017
Revised
April 25, 2017
Accepted
May 12, 2017
Published
June 01, 2017

Abstract

This paper presents a numerical analysis of magnetohydrodynamic (MHD) boundary layer flow of Jeffrey fluid over a porous unsteady shrinking sheet considering the suction parameter. The governing nonlinear partial differential equations are converted into ordinary differential equations by using a similarity approach. Numerical solutions of the nonlinear ordinary differential equations are found by using Runge-Kutta fourth order (RK4O) method with shooting technique. Effects of different parameters on velocity profiles are displayed graphically for both Newtonian (i.e.) and non-Newtonian (i.e.) flow cases. In addition, the skin friction coefficient is analyzed with the help of graphs and tables, which makes excellent agreement with the previous results. Finally, it is found that the skin friction coefficient as a function of suction parameter increases by enhancing the values of unsteady parameter while it decays by increasing the Jeffrey parameter.

***Corresponding email**: mohammadmainul.hoque@uon.edu.au (Mohammad Mainul Hoque).

DOI: https://doi.org/10.51141//IJATR.2017.3.1.1

Nomenclature

ν	Kinematic viscosity
σ	Electric conductivity of the fluid
ρ	Fluid density
λ_1	Jeffrey fluid parameter.
M	Hartmann number
β	Dimensionless unsteady parameter
S	Suction parameter
C_f	Skin friction coefficient

τ_w Skin friction

1. Introduction

The boundary layer equations play a significant role in many aspects of fluid mechanics. The steady incompressible viscous fluid over a shrinking sheet has many applications in manufacturing industries and technological process such as glass fiber production, wire drawing, paper production, metal and polymer processing industries and many others. Carane (1970) first considered the steady laminar boundary flow of a Newtonian fluid caused by a linearly stretching flat sheet and found an exact similarity solution in closed analytical form. Lok et al. (2011) discussed on magnetohydrodynamic (MHD) stagnation point flow towards a shrinking sheet. Zaimi et al. (2014) presented flow past a permeable stretching/shrinking sheet in a Nanofluid using two phase model. MHD stagnation point flow over a nonlinearly stretching/shrinking sheet was illustrated by Jafar et al. (2013). Stagnation point flow over a shrinking sheet in a micropolar fluid was discussed by Ishak (2010). Zaimi et al. (2014) discussed boundary layer flow and heat transfer over a nonlinearly permeable stretching/shrinking sheet in a nanofluid. Stagnation point flow and heat transfer of a magneto micropolar fluid towards a shrinking sheet with mass transfer and chemical reaction was established by Batool and Shraf (2013). Bhattacharyya et al. (2013) presented an exact solution for boundary layer flow of Casson fluid over a permeable stretching/shrinking sheet. Dual solutions in MHD stagnation point flow of Prandtl fluid impinging on shrinking sheet explained by Akbar et al. (2014). Effects of heat source/sink on MHD flow and heat transfer over a shrinking sheet with mass suction has been discussed by Bhattacharyya (2011). Heat transfer on MHD stagnation point flow in nanofluid past a porous shrinking/stretching sheet with variable stream condition in the presence of blowing at the surface was examined by Balachandar et al. (2015). Jain et al. (2015) analyzed effects of MHD on boundary layer flow in porous medium due to exponentially shrinking sheet with slip. Numerical solution of two-dimensional stagnation flows of micropolar fluids towards a shrinking sheet by using SOR iterative procedure was presented by Shafique et al. (2015). Very recently a number of boundary layer micropolar fluid flow studies were reported in the literature (Anika et al. 2013 & 2015) using finite difference method (FEM). Nadeem et al. (2015) analyzed MHD boundary layer flow over an unsteady shrinking sheet, by analytical and numerical approaches. Rosali et al. (2015) discussed rotating flow over an exponentially shrinking sheet with suction. Yasin et al. (2016) studied on MHD heat and mass transfer flow over a permeable stretching/shrinking sheet with radiation effect.

The significance of non-Newtonian fluids in boundary layer flow has increased due to their extensive industrial and technological applications. The usual Navier-Stokes equation flops to define the characteristics of these kinds of flows. It is worth noting that such fluids cannot be examined by a single constitutive relationship between shear stress and rate of strain (Raju et al., 2017). The non-Newtonian materials are employed in different applications associated to biological sciences, geophysics and chemical and petroleum processes (Hayat et al., 2016). The examples of non-Newtonian fluids include drilling muds, soaps, sugar solution pastes, clay coating, lubricant, certain oils, colloidal, apple sauce, foams, ketchup and suspension solutions. There are three types of non-Newtonian fluids namely differential, integral and rate types. Rate type fluids describe the impact of relaxation and retardation time. Jeffrey fluid is one of the rate type materials, which shows the linear viscoelastic effect of fluid; it has many applications in polymer industries. Hayat et al. (2012) studied the power law heat flux and heat source with Jeffrey fluid, radiation and porous medium. Hamad et al. (2013) analyzed the thermal jump effects on boundary layer flow of a Jeffrey fluid near the stagnation point with stretching/shrinking sheet and variable thermal conductivity. Farooq et al. (2015) examined the Newtonian heating in MHD flow of Jeffrey fluid. Abbasi et al. (2015) examined influence of heat and mass flux conditions in hydromagnetic flow of Jeffrey nanofluid. Reddy et al. (2015) analyzed the flow of Jeffrey fluid between torsionally oscillating disks. Many researchers (Raju et al., 2016 & 2017; Nadeem et al., 2009; Hoque et al., 2013 & 2015; Beg et al., 2014) analyzed non-Newtonian fluid characteristics over various geometries and flow characteristics.

In this study, we analyze MHD Jeffrey fluid over a porous unsteady shrinking sheet considering the effect of suction parameter. After the self-similarity transformation, the boundary governing equations are solved numerically using Runge-Kutta fourth order (RK4O) method with shooting technique (Bhukta et al., 2016; Tripathy et al., 2016). The simulations are carried out for both Newtonian ($\lambda_1 = 0$) and non-Newtonian ($\lambda_1 = 0.5$) flow cases. The variations in physical characteristics of the flow dynamics for several parameters involved in the equations are discussed in detail.

2. Mathematical Formulation

Consider the MHD boundary layer flow of an electrically conducting Jeffrey fluid over an unsteady porous shrinking sheet (Fig. 1). The time dependent magnetic field $B(t) = B_0 (1-\gamma t)^{-1}$ is applied along the direction normal to the shrinking sheet. Due to the small magnetic Reynolds number, the induced magnetic field is neglected in the present analysis. It is assumed that the x- axis is parallel to the porous surface and y-axis is normal to it. The shrinking sheet velocity $U_w(x,t) = \dfrac{-U_0\ x}{1-\gamma t}$ and wall mass transfer velocity $\upsilon_w(x,t) = -f(0)\sqrt{\dfrac{U_0 \nu}{1-\gamma t}}$ (where U_0 is a constant having a dimension of 1/time) are assumed to be varying linearly from the origin O, as shown in Fig. 1.

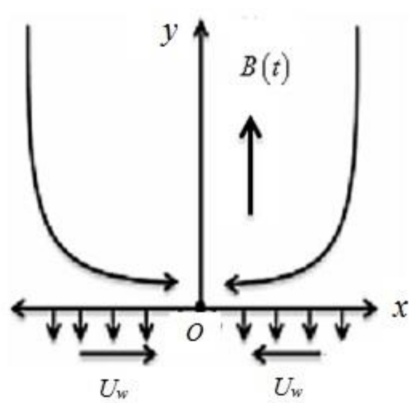

Fig. 1: Physical model of the flow (Nadeem et al., 2015).

Under the above assumptions, the governing equations of this problem can be expressed as follows (Nadeem et al., 2015):

$$\frac{\partial u}{\partial x}+\frac{\partial v}{\partial y}=0 \tag{1}$$

$$\frac{\partial u}{\partial t}+u\frac{\partial u}{\partial x}+v\frac{\partial u}{\partial x}=\frac{v}{1+\lambda_1}\frac{\partial^2 u}{\partial y^2}-\frac{\sigma B^2(t)}{\rho}u \tag{2}$$

where u and v are the velocity components along the x and y directions, respectively. $v\left(=\frac{\mu}{\rho}\right)$ is the kinematic viscosity, σ is the electric conductivity of the fluid, ρ is the density of the fluid and λ_1 is the Jeffrey parameter.

The appropriate boundary conditions of Eqs. (1)- (2) are

$$\left.\begin{aligned} &u(x,y,t)=U_w(x,t),\ \upsilon(x,y,t)=\upsilon_w(x,t)\ at\ y\to 0 \\ &u(x,y,t)=0\ as\ y\to\infty \end{aligned}\right\} \tag{3}$$

Introducing the stream function ψ, the velocity components u and v can be written as

$$u=\frac{\partial\psi}{\partial y} \text{ and } v=-\frac{\partial\psi}{\partial x} \tag{4}$$

The mass conservation Eq. (1) is satisfied automatically for Eq. (4), while the momentum Eq. (2) takes the following form

$$\frac{\partial^2\psi}{\partial y\partial t}+\frac{\partial\psi}{\partial y}\frac{\partial^2\psi}{\partial x\partial y}-\frac{\partial\psi}{\partial x}\frac{\partial^2\psi}{\partial y^2}=\frac{v}{1+\lambda_1}\frac{\partial^3\psi}{\partial y^3}-\frac{\sigma B^2(t)}{\rho}\frac{\partial\psi}{\partial y} \tag{5}$$

The corresponding boundary conditions Eq. (3) for the velocity components reduce to

$$\left.\begin{aligned} &\frac{\partial\psi}{\partial y}=U_w(x,t),\ \frac{\partial\psi}{\partial x}=-\upsilon_w(x,t)\ at\ y=0 \\ &\frac{\partial\psi}{\partial y}=0\ as\ y\to\infty \end{aligned}\right\} \tag{6}$$

Now we introducing the dimensionless variables for ψ as

$$\left.\begin{aligned} &\psi=xf(\eta)\sqrt{\frac{vU_0}{1-\gamma t}},\ \eta=y\sqrt{\frac{U_0}{v(1-\gamma t)}} \\ &u=\frac{\partial\psi}{\partial y}=\frac{U_0x}{1-\gamma t}f'(\eta),\ \upsilon=-\frac{\partial\psi}{\partial x}=-\sqrt{\frac{U_0v}{1-\gamma t}}f(\eta) \end{aligned}\right\} \tag{7}$$

With the help of Eq. (7), the self-similarity transformation of the momentum equation takes the following form

$$\frac{1}{1+\lambda_1} f''' - \left(M^2 + \beta\right) f' - \frac{\beta}{2}\eta f'' + ff'' - f'^2 = 0 \tag{8}$$

The corresponding transformed boundary conditions are

$$\left.\begin{array}{l} f = S,\ f' = -1 \ at \ \eta = 0 \\ f' \to 0 \ as \ \eta \to \infty \end{array}\right\} \tag{9}$$

where $M^2 = \dfrac{\sigma B_0^2}{\rho U_0}$ is the Hartmann number, $\beta = \gamma / U_0$ is the dimensionless unsteady parameter, $S = -\upsilon_w \left(\dfrac{1-\gamma t}{U_0 v}\right)^{1/2}$ is the suction parameter and λ_1 is Jeffrey parameter.

The quantity of the physical interest in this study is skin friction coefficient C_f , which is defined as

$$C_f = \frac{1}{1+\lambda_1}\frac{\tau_w}{\rho u_w^2} \tag{10}$$

where the skin friction τ_w is

$$\tau_w = \frac{\mu}{1+\lambda_1}\left(\frac{\partial u}{\partial y}\right)_{y=0} \tag{11}$$

Using the Eq. (7) we will get

$$\mathrm{Re}_x^{1/2} C_f = \frac{1}{1+\lambda_1}\left[f''(\eta)\right]_{\eta=0} \tag{12}$$

where $\mathrm{Re} = \dfrac{U_w x}{v}$.

3. Method of solution

Eq. (8) with the corresponding boundary conditions (Eq.9) is solved numerically using Runge-Kutta fourth order (RK4O) method with shooting technique. Initially, the nonlinear ordinary differential equation is converted to first order ordinary differential equation, by using the following procedure:

$$G' = y2, G'' = y3, G = y1, \tag{13}$$

$$G'' = (1+\lambda_1)\left\{(M^2+\beta)y_2 + \frac{\beta}{2}\eta y_3 - y_1 y_3 + {y_2}^2\right\} \tag{14}$$

With the boundary conditions as

$$\begin{aligned} &y1 = S, y2 = -1, \text{ at } \eta \to 0 \\ &y_2 = 0, \text{ at } \eta \to \infty \end{aligned} \tag{15}$$

We guess the values of $y_3(0)$, which are not given at the initial conditions. Eqs. (13)-(15) are subsequently solved using the RK4O method with shooting technique where the consecutive iterative step length is 0.01.

4. Results and Discussion

In the present study, the numerical simulations are performed for several values of dimensionless parameters such as Hartmann number *M*, Jeffrey parameter λ_1, Suction parameter S and unsteady parameter β. The variations of skin friction coefficients $\frac{f''(0)}{1+\lambda_1}$ for various values of unsteady parameter β and suction parameter S are summarized in Table 1 and 2, respectively. In the absence of Jeffrey parameter $\lambda_1 = 0$, the present results make a good agreement with Nadeem et al. [18].

Table 1: Skin friction coefficient $\frac{f''(0)}{1+\lambda_1}$ for different values of unsteady parameter β with $S = 1$ and $M = 2$

β	**Present study,** $\lambda_1 = 0$	**Nadeem et al. (2015)**
0	2.302776	2.30277
1	2.488881	2.48888

Table 2: Skin friction coefficient $\frac{f''(0)}{1+\lambda_1}$ for different values of suction parameter S with $\beta = 3$ and $M = 1$

S	**Present study,** $\lambda_1 = 0$	**Nadeem et al. (2015)**
1	2.053522	2.05352
3	3.507663	3.50767

In order to validate the present numerical results, the computed velocity profile of the present study is compared with the results reported by Nadeem et al. (2015), as shown in Fig.2. The plotted velocity profile in the absence of the Jeffrey parameter ($\lambda_1 = 0$) precisely overlaps over the velocity field of Nadeem et al. (2015), thus proving the accuracy of the present simulation. The velocity profiles over steady shrinking sheet ($\beta = 0$) for several values of suction parameter S are depicted in Fig 3 considering both Newtonian ($\lambda_1 = 0$), non-Newtonian ($\lambda_1 = 0.5$) cases. It is evident that momentum boundary layer thickness is enhanced by increased S.

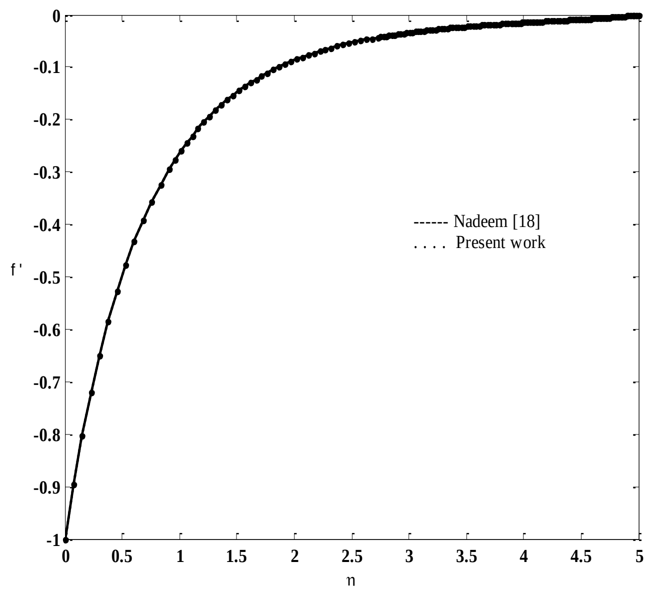

Fig. 2: Velocity profile when $S = -0.5,\ \beta = 1$ and $M = 2$.

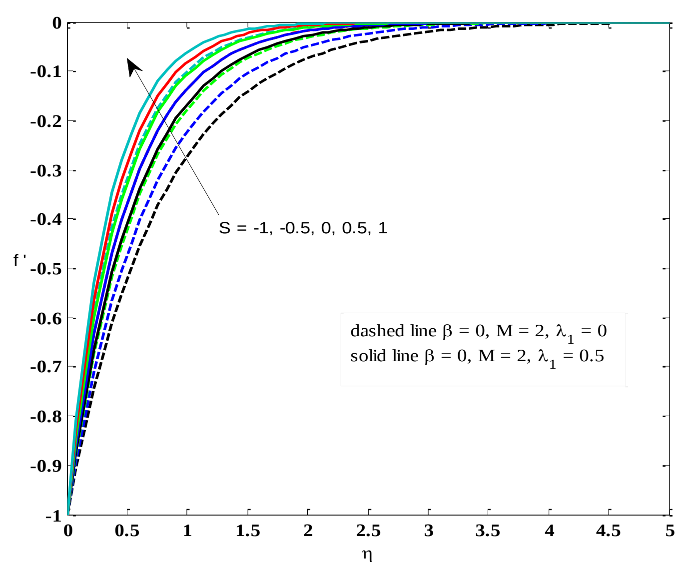

Fig. 3: Velocity profile for several values of S.

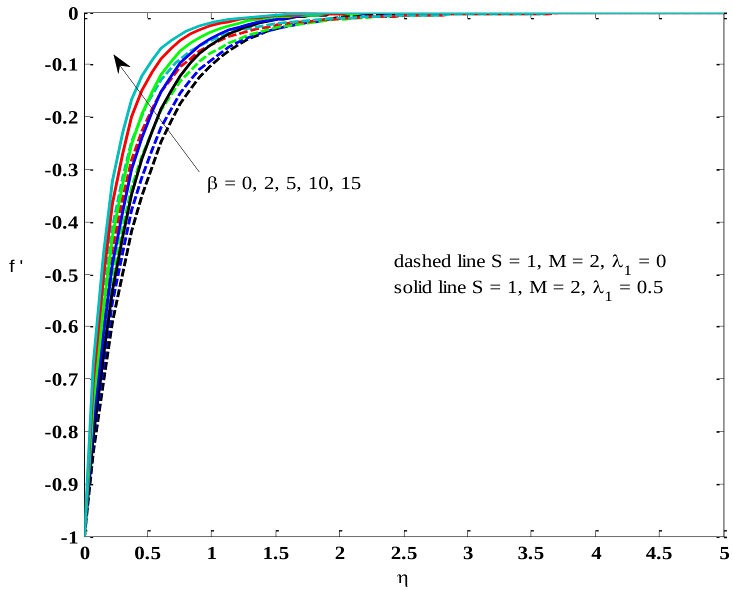

Fig. 4: Velocity profiles for several values of β.

Fig. 4 shows the effect of unsteady shrinking sheet parameter β on the velocity profile for both Newtonian and non-Newtonian cases. It is clear that the velocity increases with increasing values of unsteady parameter β and consequently the boundary layer thickness decreases by increase of β. The influence of Hartmann number M on the velocity profiles for both Newtonian and non-Newtonian cases is shown in Fig 5. It is noticed that the velocity increases with increasing M and consequently the boundary layer thickness decreases. Physically the present phenomenon occurs when magnetic field induces current into the conductive fluid creating a resistive type force in the fluid within the boundary layer that shows down the moment of the fluid. Hence, the magnetic field is used to control the boundary layer separation.

The velocity profiles for several values of Jeffrey parameter λ_1 is shown in Fig 6. It is noticed that with increase of λ_1, the velocity increases and consequently the boundary layer thickness decreases. The variation of skin friction coefficient as a function of suction parameter S for different values of β and λ_1 are plotted in Fig. 7 and Fig. 8 respectively. It is noticed that the skin coefficient increases with increasing values of β while a reverse behavior is also observed for different values of λ_1. It is worth to note that these observation makes an excellent agreement with Nadeem et al. (2015).

3. Conclusions

In the present study, MHD boundary layer flow of Jeffrey fluid over a porous unsteady shrinking sheet has been investigated using the RK4O method associated with shooting technique. It is found that the velocity profile enhances by increasing the values of Hartmann number M, Jeffrey parameter λ_1, suction parameter

S and unsteady parameter β, for both Newtonian and non-Newtonian cases. The skin friction coefficient as a function of suction parameter increases by enhancing the values of β while it decays by increasing λ_1. In addition, the present study accords well with the results of Nadeem et al. (2015) in the absence of Jeffrey parameter. In future, the effect of gyrotactic microorganism on the Jeffery fluid over a porous shrinking sheet will be investigated following the work of Raju et al. (2017).

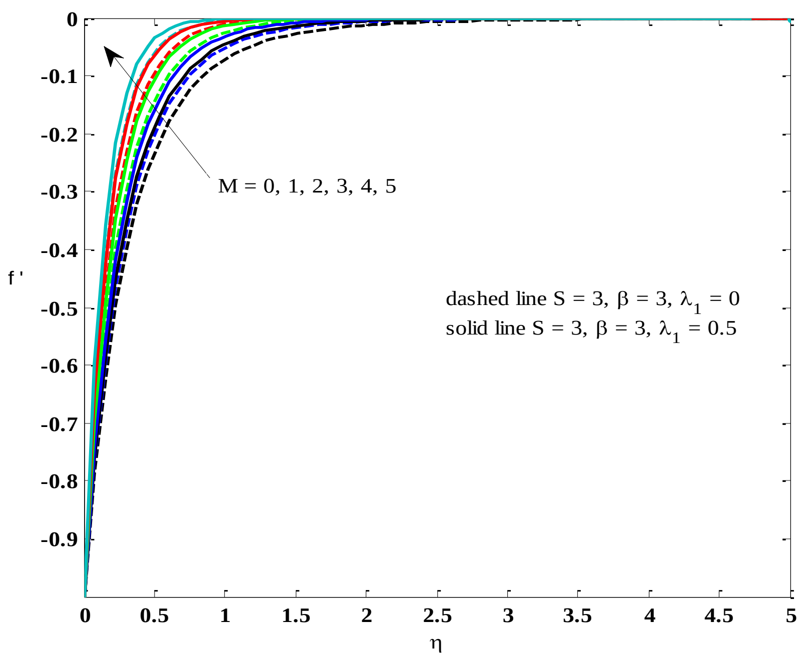

Fig. 5: Velocity profiles for several values of M .

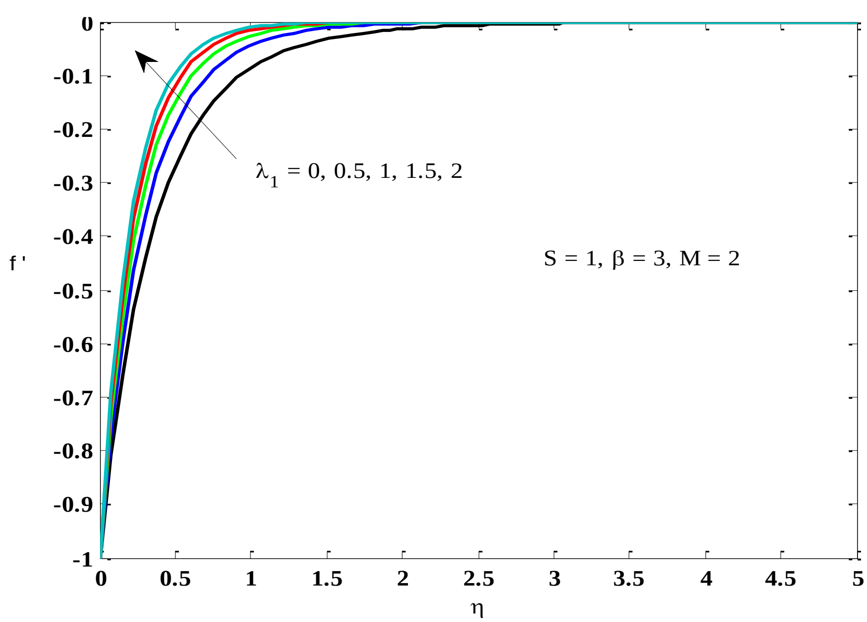

Fig. 6: Velocity profiles for several values of λ_1.

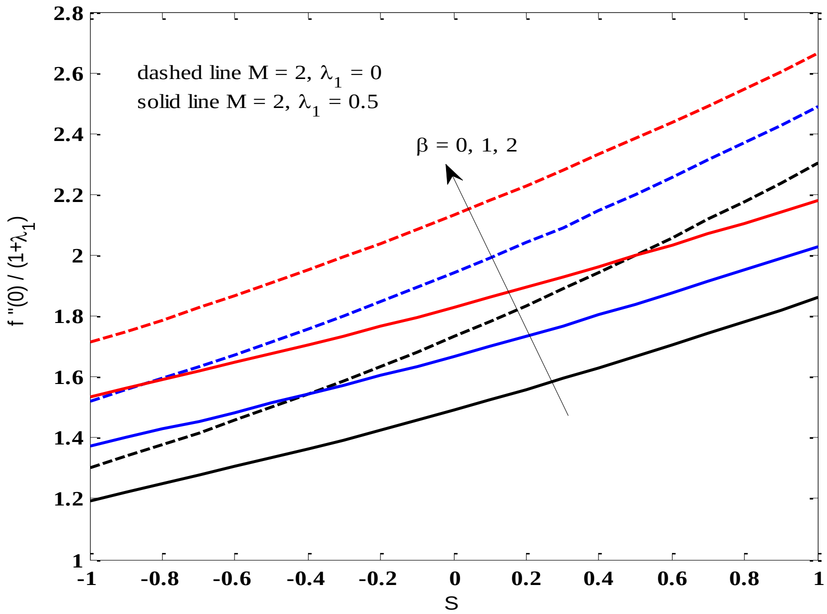

Fig. 7: Skin friction coefficient for several values of β against S.

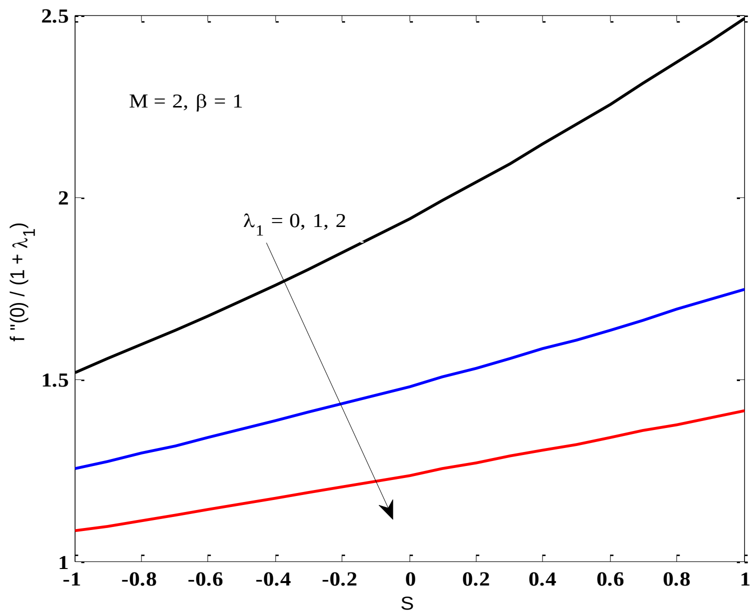

Fig. 8: Velocity profiles for several values of λ_1 against S.

References

Abbasi FM, Shehzad SA, Hayat T, Alsaedi A, Obid MA. (2015). Influence of heat and mass flux conditions in hydromagnetic flow of Jeffrey nanofluid, AIP Advances 5: 037111.

Akbar NS, Khan ZH, Haq R, Nadeem S. (2014). Dual solutions in MHD Stagnation-point flow of prandtl fluid impinging on shrinking sheet, Applied Mathematics and Mechanics 35(7):813-820.

Anika NN, Hoque MM, Hossain S, Alam MM. (2015). Thermal diffusion effect on unsteady viscous MHD micropolar fluid flow through an infinite plate with hall and Ion-slip current, Procedia Engineering 105:160–166.

Anika NN, Hoque MM, Islam N. (2013). Hall current effects on Magnetohydrodynamics fluid over an infinite rotating vertical porous plate embedded in unsteady laminar flow, Annals of Pure and Applied Mathematics 3(2): 189-200.

Anika NN, Hoque MM. (2013). Thermal buoyancy force effects on developed flow considering hall and ion-slip current, Annals of Pure and Applied Mathematics 3(2): 179-188.

Anika NN, Hoque MM, Alam MM. (2013). Unsteady free convection flow with flow control parameter, Current Trends in Technology and Science, 2(1):193-201.

Balachandra VV, Hasan SB, Kandasamy R. (2015). Heat transfer on MHD stagnation point flow in nanofluid past a porous shrinking/stretching sheet with variable stream condition in the presence of blowing at the surface. Journal of Mechanical Engineering Research 7(3):22-33

Batool K, Shraf MA. (2013). Stagnation point flow and heat transfer of a magneto micropolar fluid towards a shrinking sheet with mass transfer and chemical reaction, Journal of Mechanics 29(3):411-422.

Beg OA, Hoque MM, Wahiduzzaman M, Alam MM, Ferdows M. (2014). Spectral numerical simulation of Mageneto-Physiological laminar Dean flow, Journal of Mechanics in Medicine in Biology 14(4) ID-1450047.

Bhattacharyya K. (2011). Effects of heat source/sink on MHD flow and heat transfer over a shrinking sheet with mass suction. Chemical Engineering Research Bulletin 15(1), 12-17.

Bhattacharyya K, Hayat T, Alsaedi A. (2013). Exact solution for boundary layer flow of Casson fluid over a permeable stretching/shrinking sheet, Journal of Applied Mathematics and Mechanics 94:522-528.

Bhukta D, Mishra SR, Hoque MM. (2016). Numerical simulation of heat transfer effect on Oldroyd 8-constant fluid with wire coating analysis, Engineering Science and Technology, an International Journal 19(4):1910-1918.

Crane LJ. (1970). Flow past a stretching plate, Zeitschrift fiir Angewandte Mathematik and Physik 21(4):645-647.

Farooq M, Gull N, Alsaedi A, Hayat T. (2015). MHD flow of a Jeffrey fluid with Newtonian heating, Journal of Mechanics 33:1–11.

Hayat T, Qayyum S, Imtiaz M, Alsaedi A. (2016). Impact of Cattaneo-Christov heat fluix in Jeffrey fluid flow with homogeneous-homogeneous reactions, PLOS one 11(2).

Hayat T, Shehzad SA, Qasim M, Obaidat S. (2012). Radiative flow of Jeffrey fluid in a porous medium with power law heat flux and heat source. Nuclear Engineering Design 243:15–19.

Hamad MAA, Gaied SMA, Khan WA. (2013). Thermal jump effects on boundary layer flow of a Jeffrey fluid near the stagnation point on a stretching/shrinking sheet with variable thermal conductivity, Journal of Fluids 749271.

Hoque MM, Alam MM, Ferdows M, Beg OA. (2013). Numerical simulation of Dean number and curvature effects on Magneto-Bio-Fluid flow through a curved conduit, Proceedings of the Institution of Mechanical Engineers, Part H, Journal of Engineering in Medicine 227(11):1155-1170.

Hoque MM, Anika NN, Alam MM. (2013). Magnetic effects on direct numerical solution of fluid flow through a curved pipe with circular cross section, European Journal of Scientific Research 103(3):343-361.

Hoque MM, Alam MM. (2013). Effects of Dean Number and curvature on fluid flow through a curved pipe with magnetic field, Procedia Engineering 56:245–253.

Hoque MM, Anika NN, Alam MM. (2013). Numerical Analysis of Magnetohydrodynamics Flow in a Curved Duct, International Journal of Scientific and Engineering Research 4(7):607-617.

Hoque MM, Alam MM. (2015). A numerical study of MHD laminar flow in a rotating curved pipe with circular cross section, Open Journal of Fluid Dynamics 5:121–127.

Ishak A, Lok YY, Pop I. (2010). Stagnation point flow over a shrinking sheet in a micropolar fluid, Chem. Eng. Communications 197:1417-1427.

Jafar K, Ishak A, Nazar R. (2013). MHD stagnation- point flow over a nonlinearly stretching/shrinking sheet, Journal of Aerospace Engineering 26(4):829-834.

Jain S, Choudhary R. (2015). Effects of MHD on boundary layer flow in porous medium due to exponentially shrinking sheet with slip, Procedia Engineering 127: 1203-1210.

Lok YY, Ishak A, Pop I. (2011). MHD stagnation-point flow towards a shrinking sheet, Int. J. of Numerical Methods for Heat & Fluid Flow 21(1):61- 72.

Nadeem S, Haq R, Lee C. (2015). MHD boundary layer flow over an unsteady shrinking sheet: analytical and numerical approach, J Braz. Soc. Mech. Sci. Eng. 37:1339-1346.

Nadeem S, Hussain A, Khan M. (2009). Stagnation flow of a Jeffrey fluid over a shrinking Sheet, Z. Naturforsch 65:540-548.

Raju CSK, Hoque MM, Sivasankar T. (2017). Radiative flow of Casson fluid over a moving wedge filled with gyrotactic micoorganisms, Advanced Powder Technology 28(2):575-583.

Raju CSK, Babu MJ, Sandeep N. (2016). Chemically reacting radiative MHD Jeffrey nanofluid flow over a cone in porous medium, International Journal of Engineering Research in Africa 19:75-90.

Raju CSK, Sandeep N. (2017). Unsteady Casson nanofluid flow over a rotating cone in a rotating frame filled with ferrous nanoparticles: A Numerical study, Journal of Magnetism & Magnetic Materials 427: 216-224.

Reddy GB, Sreenadh S, Reddy RH, Kavitha A. (2015). Flow of a Jeffrey fluid between torsionally oscillating disks, Ain Shams Engineering Journal 6:355–362.

Rosali H, Ishak A, Nazar R, Pop I. (2015). Rotating flow over an exponentially shrinking sheet with suction, Journal of Molecular Liquids 211:965-969.

Shafique M, Nazir A, Abbas F. (2015). Numerical solution of two-dimensional stagnation flows of micrioplar fluids towards a shrinking sheet by using SOR iterative procedure, Journal of Progressive Research in Mathematics 3(1):131-139.

Tripathy RS, Dash GC, Mishra SR, Hoque MM. (2016). Numerical analysis of hydromagnetic micropolar fluid along a stretching sheet embedded in porous medium with non-uniform heat source and chemical reaction, Engineering Science and Technology, an International Journal 19(3):1573-1581.

Yasin MHM, Ishak A, Pop I. (2016). MHD heat and mass transfer flow over a permeable stretching/shrinking sheet with radiation effect, Journal of Magnetism and Magnetic Materials 407:235-240.

Zaimi K, Ishak A, Pop I. (2014). Flow past a permeable stretching/shrinking sheet in a nanofluid using two phase model, Plos one 9(11):1-6.

Zaimi K, Ishak A, Pop I. (2014). Boundary layer flow and heat transfer over a nonlinearly permeable stretching/shrinking sheet in a nanofluid, Scientific Reports 4404:1-8.